Case Studies in Construction Materials 15 (2021) e00611

Contents lists available at ScienceDirect

Case Studies in Construction Materials

journal homepage: www.elsevier.com/locate/cscm

Case study

Green composite plaster with modified morphology for enhanced thermal comfort in buildings

K.A.D.Y.T. Kahandawa Arachchi [a,*], A. Selvaratnam [a], J.C.P.H. Gamage [a], G.I. P. De Silva [b]

[a] Department of Civil Engineering, University of Moratuwa, Sri Lanka
[b] Department of Material Science and Engineering, University of Moratuwa, Sri Lanka

ARTICLE INFO

Keywords:
Waste material
Bottom ash
Morphology
Composite plaster
Thermal comfort
Tropical exposure
FEM

ABSTRACT

Partially replacement of constituent materials in cementitious products using waste materials leads to reduce the CO_2 emissions while saving the natural resources and minimize the environmental hazards caused by waste disposal. Development of such an alternative for conventional plaster with better thermal performance, strength and durability characteristics will result in energy savings in the construction and operational phases of buildings.

A composite plaster was developed by dry mixing of fine aggregate, bottom ash (BA), Portland cement and poly-carboxylic ether-based admixture. Their phase composition and microstructure morphologies were evaluated using XRD and SEM for a range of compositions and comparisons were made by varying water to cement ratios on the development of the best composition. The results indicate that the morphology and grain dimensions of the developed composite plaster can save 60 % of fine aggregate with effective replacement of bottom ash while maintaining the water to cement ratio of 1.15. A reduction of thermal conductivity by 76 % was noted concerning to the conventional plaster. The application of this waste based composite plaster in model units indicated good adhesion properties with better surface texture and good water resistance characteristics. No thermal or shrinkage cracks appeared in the operational phase of the models under outdoor exposure of two years to the tropical environment. A numerical model was also developed to predict the indoor wall temperature variation of a compartment finished with the said composite plaster and a comparison was made with the measured temperature cycle during outdoor exposure. A parametric study was conducted to compare the heat balance of the developed models with available systems and different climate variations.

1. Introduction

Exploiting the reusability of waste materials is a prevalent research area. In a world where power generation plays a prominent role, waste accumulation through power generation often raises several concerns [1]. The coal generates nearly 40 % of the world's electricity in 2020 [2]. Fly ash and bottom ash (BA) are the two main byproducts accumulated through this process [3,4]. Even though fly ash has found its utility as a replacement for cement in construction industry applications [5], the uses of BA are still being explored.

Using BA in light weight concrete [6] and thermal insulation blocks [7] are currently researched upon. However, using BA for

* Corresponding author.
E-mail address: tharikakahandawa@gmail.com (K.A.D.Y.T. Kahandawa Arachchi).

https://doi.org/10.1016/j.cscm.2021.e00611
Received 24 April 2021; Received in revised form 25 June 2021; Accepted 30 June 2021
Available online 3 July 2021

fashioning geo-polymer products or as a replacement for cement has rendered it impossible due to its nature of coarse particles, and presence of high carbon content and heavy metal content [3]. Therefore, BA is generally exploited as a partial replacement for fine aggregates of cementitious materials [8]. Moreover, owing to the porous nature of the particles and high water absorption, replacement of BA exerts an adverse effect on the compressive strength of the mixture [9]. Nevertheless, this porous nature can be advantageous when it comes to developing an insulation material [10]. However, being a byproduct of the burning process of coal, the chemical and mechanical properties of BA vary with the origin and burning process of the power plant which must be taken into account before the investigation [3,11].

The applicability of cementitious insulation materials on buildings often incorporates the indoor thermal comfort of the building. Over the years, attempts have been made to develop insulation materials using both organic and inorganic compounds [12,13]. Rice husk ash [14,15], EPS [16,17], Natural fibers [18] etc. have been researched as cementitious insulation materials. Reduction of heat penetration through walls leads towards maximizing the comfort as well as minimizing the energy usage in buildings [19]. In addition, the reduction of energy usage would lead towards a more economical solution in case of power usage.

Thermo-mechanical properties of BA have been researched upon before. However, no study has been done on developing an appropriate combination of materials for a cementitious insulation system using bottom ash and the feasibility of the material in application as wall plaster on buildings. This study is focused on developing the perfect combination sequence for an external plaster, its feasibility of application in buildings during short term and long-term performance. A comparative study on heat transfer behavior of the newly developed composite wall is also included.

2. Experimental study

The test program for the development of a cementitious insulation plaster can be broadly categorized into two areas; investigation of chemical and physical properties of BA for feasibility analysis and investigation of mechanical and physical properties of developed cementitious plaster. Fig. 1 presents a detailed progress of the test series to develop an insulated plaster using BA.

3. Chemical and physical properties of Bottom ash (Phase 1)

Literature suggests that there can be a differentiation in thermal conductivity of BA with its chemical and physical properties [3, 20]. Phase 1 was conducted to address this concern. The morphology- nature of the particles and their distribution, was observed using a Scanning Electron Microscope (SEM) –Model "Zeiss EVO 18 research". An atomic absorption spectrometer was used for analysing the chemical composition of BA. Furthermore, X-Ray Diffraction (XRD) was carried out using the "BRUKER ECO D8 advance diffractometer" to observe the peak patterns correspond to different types of mineral phases present in the BA sample.

3.1. SEM imaging

The morphologies of Brazilian [21] and Norochcholai BA (current study) are shown in Fig. 2-(a) and -(b), respectively. According to the Fig. 2-(a), Brazilian BA consists of higher percentage of round shaped particles compared to the Norochcholai BA. Furthermore, surface morphology of the Norochcholai BA (Fig. 2-(b)) showed more porous particles relative to the Brazilian BA. In the case of a porous material, its thermal conductivity relies upon the geometrical distribution of the void phases (i.e. pore structure) and volume

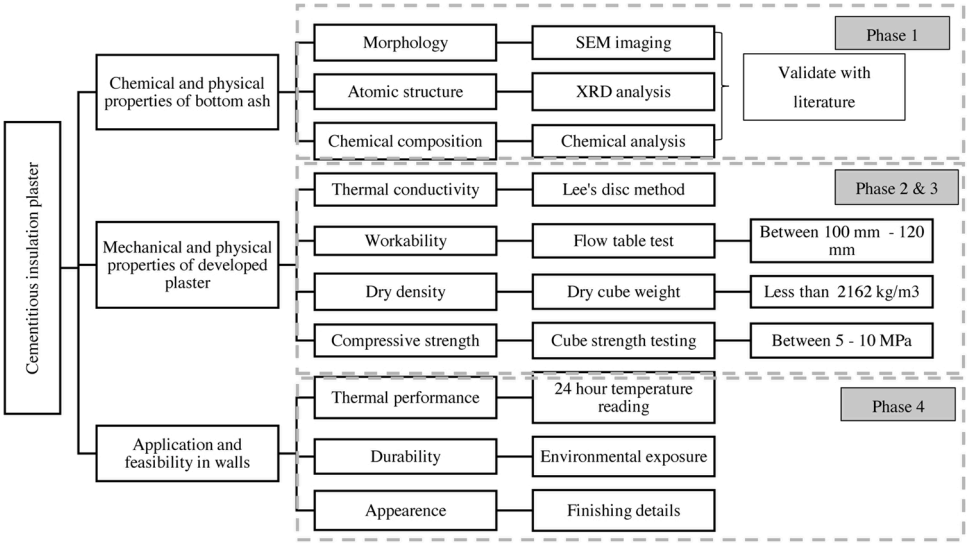

Fig. 1. Overview of the program.

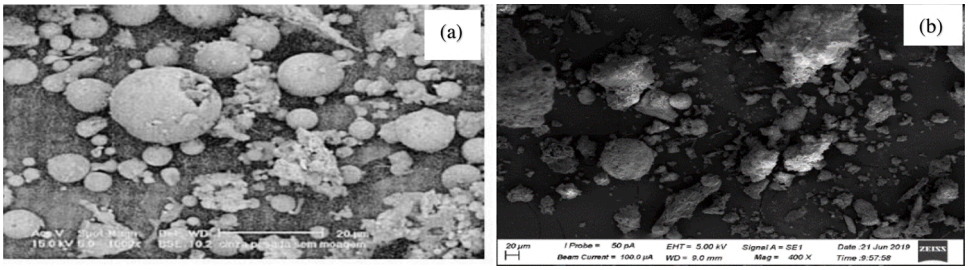

Fig. 2. Morphology a) Literature [21] b) Current study.

fraction of its solid constituents [22].

3.2. XRD analysis

The XRD results of the BA samples from Russia [23] and from Norochcholai power plant (current study) are shown in Fig. 3-(a) and (b), respectively. Quartz (SiO_2), mullite and Aluminum oxide (Al_2O_3) crystalline phases were dominantly appeared in XRD spectra of Norochcholai sample whereas Quartz (SiO_2) and Calcite ($CaCO_3$) were identified in sample from Russia. These results show that Norochcholai BA has shown significant variation with sample from Russia. However, it was revealed that the XRD results of Norochcholai BA sample are closer to the generally accepted XRD results of BA [21,23] in terms of crystalline phases, diffraction peak positions (2θ) and their intensities. Moreover, literature [24] suggests that, infused BA structure, Mullite phase reduces the thermal conductivity than the quartz structure of river sand.

3.3. Chemical analysis

When the chemical composition of BA is considered, literature suggests that major components are silica, alumina and iron oxide [6,21,25]. However, the byproduct of a combustion process tends to differ from each other due to various environmental factors. For

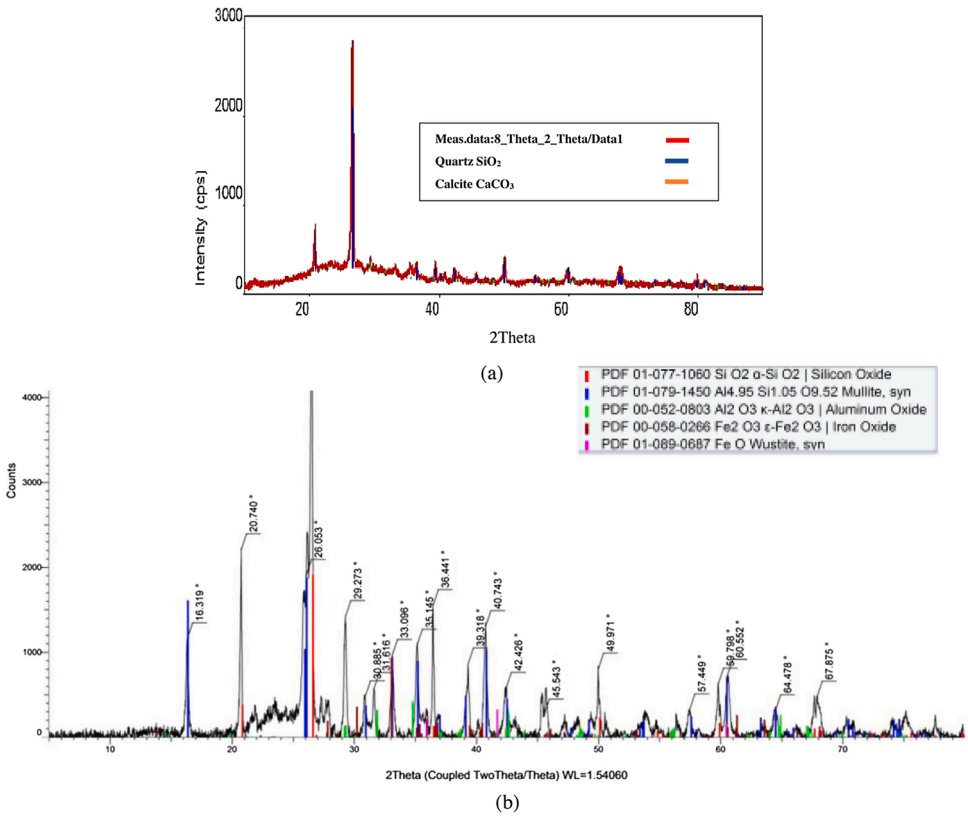

Fig. 3. XRD Imaging (a) Literature [23] (b) Current study.

example, the coal for the Norochcholai power plant is imported from Indonesian ores. The process of coalification itself suggests that the composition of coal could vary with the dead vegetation that involves in the process. Therefore, Table 1 shows slightly different compositions for BA samples obtained from Russia, Brazil and Norochcholai power plants. The chemical composition of sand comprises more than 90 % of SiO_2. However, the results in Table 1 shows that the % of Silica (SiO_2) in BA is around 50 % and around 25 % is Alumina (Al_2O_3). The research of McQuarrle [26] shows that the thermal resistivity of Al_2O_3 increases at elevated temperatures. Thereby, as the decrease of SiO_2 in BA than sand is mainly fulfilled by Al_2O_3, it could be a reason for improved insulation properties of BA.

4. Development of the plaster

The test program for obtaining optimum mix proportions were carried out as a trial and error program.

4.1. Materials

Ordinary Portland Cement (OPC) with 28-day compressive strength of 42.5 MPa [27] was used as the basic cementitious material for all the mixtures (Fig. 4). Table 2 gives the material properties of the constituents.

4.2. Sample preparation

Initially, the control plaster samples were cast using the proportions of sand/cement ratio of 3 and water/cement ratio of 0.6 to match with the common industry practice for N – type plaster. Ten different mix proportions were selected with a variation of BA in the range from 0 to 100% (Table 3). Water absorption of BA was not obtained. Therefore, both BA and river sand were oven-dried to avoid water absorption dispersion from aggregates to the mixture. The materials were mixed using a mechanical mixer for 5 min prior to adding water. Then the plaster was further mixed for 10 min after adding water (Fig. 5-(a)).

4.2.1. Test samples for thermal conductivity

Samples with 5 mm thickness and 60 mm diameter (Fig. 5-(b)) were cast. Their thermal conductivities were tested using the Lee's disc method (Fig. 5-(c)), in accordance with ASTM D7340 – 07 [28].

4.2.2. Test samples for compressive strength

After measuring the thermal conductivity, three best proportions were selected. Cement cubes were prepared from selected proportions to measure the compressive strength (Fig. 5-(d)) in accordance with ASTM C109 [29].

4.3. Mechanical and physical properties of the plaster (Phase 2,3)

The procedure for determining the mechanical and physical properties is presented in Fig. 6. This was conducted in two phases. The mechanical properties of the developed plaster were validated with the standards for type N plaster [30].

The experimental results for thermal conductivity and compressive strength are given in Table 4. Fig. 7 shows the variation of thermal conductivity and compressive strength with the % of BA in the mix.

Three mix proportions were isolated from the above samples, namely 50 %, 60 %, 70 % and then tested for their compressive strength at 7 days (Table 4) (Fig. 7). The average compressive strength of the samples decreases with the increased BA replacement in the samples. This is mainly due to the increased porosity resulted from increased percentage of BA.

The workability of the mix proportions were measured according to ASTM C1437−20 [31]. The compressive strength and workability drastically decreased with the addition of BA to the plaster. Therefore, compressive strength testing was repeated with increasing water/cement ratios for the selected mix designs to achieve an optimum w/c ratio (Table 5, Fig. 8).

Table 1
Chemical analysis results of different bottom ash samples.

Oxide	Brazil [21] Percentage %	Russia [23] Percentage %	Sri Lanka (Current Study) Percentage %
SiO_2	56.0	55.7	48.23
Al_2O_3	26.7	21.83	19.39
Fe_2O_3	5.8	7.44	3.61
MgO	0.6	1.95	1.33
CaO	0.8	6.8	7.74
Na_2O	0.2		0.95
FeO	–	6.69	–
K_2O	2.6	3.53	0.62
TiO_2	1.3	1.11	1.18
S	0.1	–	–
P_2O_5	–		1.16
SO_3	–	0.72	–

Fig. 4. Materials - a) Cement b) Sand c) Bottom ash.

Table 2
Material properties.

	Cement	River sand	Bottom ash
Specific gravity	3.15	2.68	1.7
Used aggregate size (mm)	< 2.36	< 2.36	< 2.36
Bulk density (kN/ m^3)	1442	1484	624

Table 3
Plaster mix proportions.

Sample	% replacement of sand by BA to weight	BA (g)	Cement (g)	Water (g)	Fine aggregate (g)
BA0	0	0	50	30	150
BA10	10	15	50	30	135
BA20	20	30	50	30	120
BA30	30	45	50	30	105
BA40	40	60	50	30	90
BA50	50	75	50	30	75
BA60	60	90	50	30	60
BA70	70	105	50	30	45
BA80	80	120	50	30	30
BA90	90	135	50	30	15
BA100	100	150	50	30	0

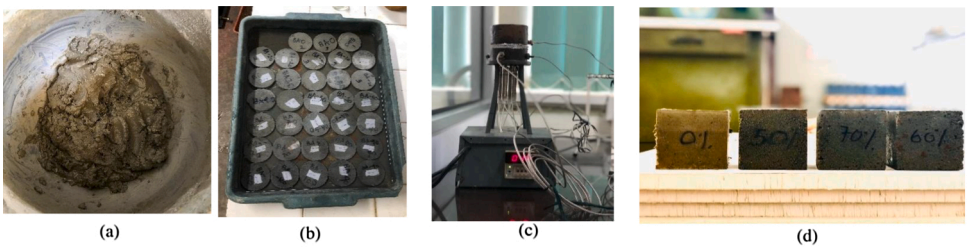

Fig. 5. (a) Mixing using the mechanical mixer (b) Thermal conductivity samples (c) Lee's disc apparatus (d) Cube test.

The compressive strength of cement plasters is supposed to decrease when w/c increases. However due to the porous nature and high water demand of BA [9] along with high yield when compared to conventional fine aggregates, the workability and strength of the plaster was increased and then decreased when it surpassed 1.2 (Fig. 8).

Considering the workability and consistency of the plaster, a superplasticizer was added as given in Table 6. The strength and workability of the samples was increased up to general working standards of the industry. The mix design with 60 % replacement of BA with 10 mL per kg of cement and 1.2 w/c ratio was selected as the optimum combination. Hereafter, the improved mix will be addressed as BA60-S.

5. Application and feasibility in walls (Phase 4)

Two model house units of size 750 mm (width) x900 mm (length) x750 mm (height) were developed to understand the general applicability quality of finishing and service performance under exterior environmental exposure of plaster. Wall thickness was 100 mm. One unit was applied with the conventional plaster (Cement: Sand 1:5) and the other was finished with the plaster of BA60-S, for a thickness of 20 mm. The models were kept in the outdoor environment and observed for a period of 6 months. The walls were exposed to daily temperature variations and the rainfall. Fig. 9- (a) shows the development of house units and application of the two types of

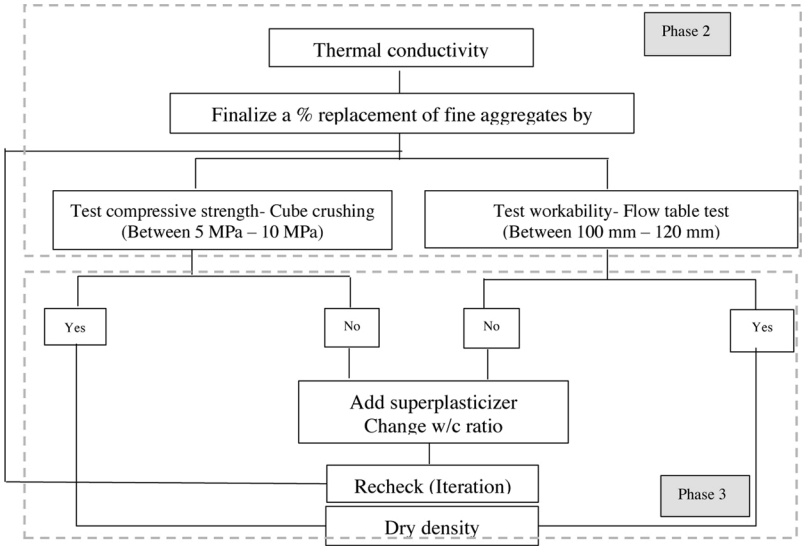

Fig. 6. Development of insulated plaster.

Table 4
Results: Mechanical properties.

% of BA replacing sand to weight	Thermal Conductivity (W/mK)	Avg. Compressive strength (N/mm^2)
0	1.44	–
10	1.36	–
20	1.15	–
30	1.24	–
40	0.99	–
50	0.82	4.41
60	0.8	3.62
70	0.7	4.11
80	0.5	–
90	0.43	–
100	0.39	–

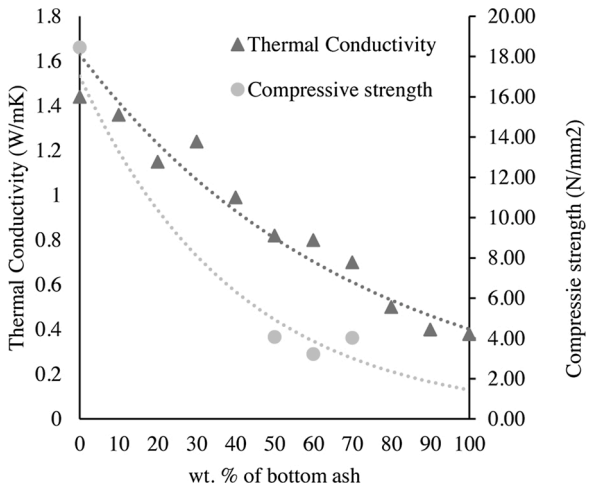

Fig. 7. Variation of thermal conductivity and compressive strength with %BA.

plaster; conventional cement-sand plaster and BA plaster.

Both improved BA60-S and conventional plaster indicated a good surface texture with proper adhesion for block wall as shown in Fig. 9-(b)). At the end of 6-month period, no signs of either thermal or shrinkage crack, spalling of plaster were noted (Fig. 9-(b)), even

Table 5
Average strength and flow variation of BA60.

w/c ratio	Average 7-day Strength (N/mm^2)	Average flow (mm)
0.6	3.6	–
0.8	6.4	–
1	9.01	88.5
1.2	10.25	150
1.4	6.17	180
1.6	4.27	220

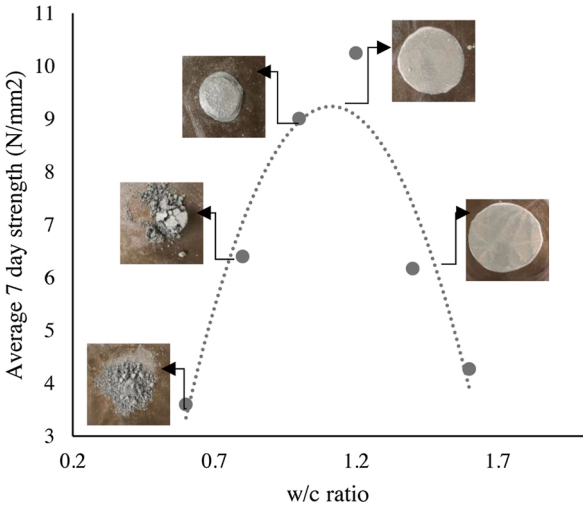

Fig. 8. Variation of compressive strength of BA60 with w/c ratio.

Table 6
Plaster mix proportions and test results.

Sample	Cement (Kg)	Fine Aggregate (Kg)	BA (Kg)	w/c Ratio	Admixture (ml per Kg of Cement)	Average Strength 28 day (N/mm^2)	Average Density (Kg/m^3)	Average Flow (mm)
BA50	1	1.5	1.5	0.8	0	2.76	1562	95
BA50	1	1.5	1.5	1	0	21.77	1842	123
BA50	1	1.5	1.5	1	10	9.96	1763	147.5
BA50	1	1.5	1.5	1	12	11.32	1856	142.5
BA60	1	1.2	1.8	1	0	9.83	1713	97.5
BA60	1	1.2	1.8	1.2	10	5.08	1712	175
BA60	1	1.2	1.8	1.2	12	8.95	1725	150

Fig. 9. a) Development of model house units b) House units after 6 months.

if the plastered model unit was exposed to dry-wet cycles in the exterior environment. This shows the practical feasibility of developed plaster for application in external walls.

6. Heat transfer analysis

6.1. Summary of test program

The plastered units were also used to validate the heat transfer model developed using a commercially available finite element software [32]. After ensuring the durability, the surface temperature of the interior and exterior walls was monitored using K-type thermocouples fixed to the surfaces (Fig. 10) for four daily consequential environmental changes. The surface temperatures were observed for peak 6 h are shown in Fig. 12.

6.2. Heat transfer modeling

A three-dimensional finite element model was developed using an advanced finite element software [32]. The heat transfer through the plastered block wall with the dimensions 3m × 4m x 0.1 m (height x length x thickness) was considered for this study. The test results indicated BA60 as the optimum mix proportions for better thermal and mechanical performance. Hence, it was chosen to analyze the heat transfer behavior through this composite wall panel.

An 8-node linear heat transfer brick elements (DC3D8) were used to model both wall and plaster elements. From a mesh sensitivity analysis, the mesh size was decided as 15 mm and the selected aspect ratios for the wall and the plaster was 1:1. Since the plaster and the wall panels are assumed as perfectly bonded, a tie constraint was used to represent its bond behavior. The developed finite element mesh of the wall panel with plaster is shown in Fig. 11.

The thermal performance of the masonry wall is to be evaluated based on two parameters; *decrement factor* and *time lag*. The decrement factor is defined as the reduction ratio in the amplitude of the temperature wave at the indoor surface compared to the outdoor surface. The time takes for the temperature wave to propagate from the outer surface to the inner surface is named as the time lag [33]. The decrement factor (f) and the time lag ($t_{\emptyset}$) can be computed using equations 1 & 2, respectively [33].

$$t_{\emptyset} = t_{E-max} - t_{I-max} \tag{1}$$

$$f = \frac{T_{I-max} - T_{I-min}}{T_{O-max} - T_{O-min}} \tag{2}$$

Where $t_{E\text{-}max}$, $t_{I\text{-}max}$, $T_{I\text{-}max}$, $T_{I\text{-}min}$, $T_{O\text{-}max}$, and $T_{O\text{-}min}$ represent the time taken to reach the maximum temperature in exterior, and interior surface; inside maximum, inside minimum, outside maximum, and outside minimum surface temperatures, respectively. The model was initially analyzed for three cases and the wall panel configurations are shown in Table 7 and the properties used for simulations are listed in Table 8.

6.3. Model results and validation

In order to validate the numerical model, the same environmental conditions for consecutive 24 h have been applied to the external wall in both models and the internal temperature variations have been monitored. The results obtained from the numerical model are illustrated in Fig. 12 along with the test results. The comparison between the test results and the predicted results shows a good agreement and the average deviation of predicted values were less than 10 %.

In order to predict the thermal performance of the composite wall throughout a day, the model was further analyzed for three consecutive days. The initial temperature at the internal wall surface was assumed as 25 °C and the model was running for a cyclic temperature for 3 days to ensure the convergence of the internal temperature variation. The applied temperature at the external surface and the obtained temperature for the internal surface of WP_BA0 are plotted in Fig. 13. Then, the temperature variation within the 24 h was extracted from the model results after the convergence of the internal variation (Fig. 14).

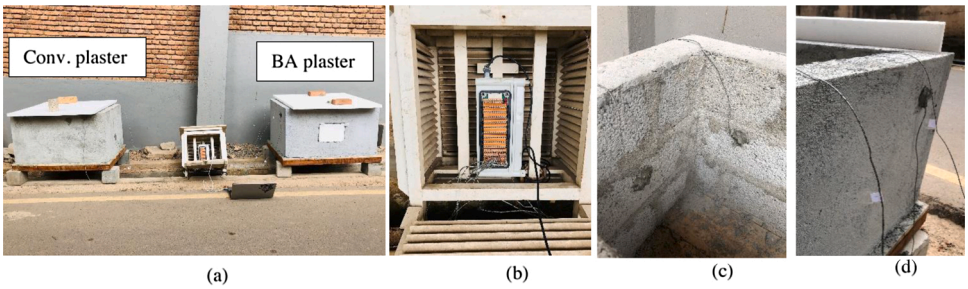

Fig. 10. a) Temperature monitoring setup b) Data logger c) Thermocouple positions inside d) Thermocouple positions outside.

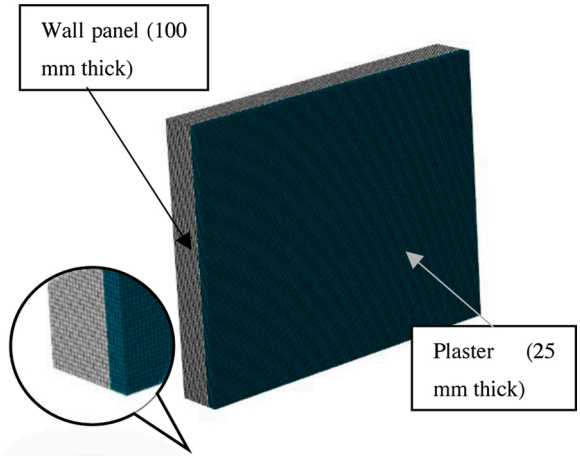

Fig. 11. Finite element mesh of the wall panel with plaster.

Table 7
Model configurations.

Model ID	Descriptions
WP_0	Wall panel without plaster
WP_BA0	Wall panel with cement-sand plaster (BA0)
WP_BA60-S	Wall panel with BA mixed plaster (BA60)[a]

[a] The best mix proportion with good thermal & strength performance.

Table 8
Thermal properties of the materials used for Finite element modeling.

Material	Measured thermal conductivity (W/m.K)	Measured specific heat (J/kg.K)	Measured density (kg/m^3)
Concrete block [37]	1.37	840	2778
Conventional plaster (BA0)	1.45	1500	2162
Plaster developed in this study (BA60-S)	0.7	900	1712

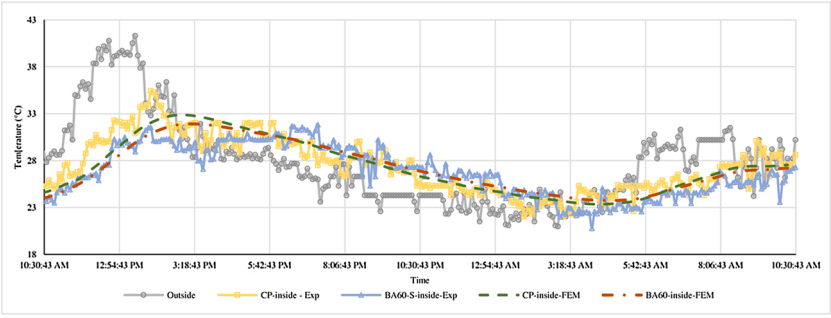

Fig. 12. Model results and validation.

Fig. 14 shows the internal and external temperature of walls for different conditions for period of a 24 h. According to the graphs, the wall with the innovative plaster shows better thermal performance. The decrement factor of the wall was observed as 0.85 without any application of the plaster (WP_0). The time lag in the wall panel model without plaster was noted as 2 h and 27 min. Shaik et al. [34] have also investigated the heat transfer behavior of building walls exposed to the periodic temperature profile and the noted decrement factor for 100 mm thick concrete block walls was 0.86 and 2 h 30 min. The similarity in these results adds further evidence of the accuracy of the heat transfer model developed in this study. By applying the conventional plaster (WP_BA0), the decrement factor of the composite wall was reduced by 9.5 %. Further, 20 % reduction was noted in the composite wall with the application of the plaster (WP_BA60-S) developed in this study which shows the improved thermal performance. The time lags in the models with plaster increased by 30.6 %, and 55.1 % of the wall panels WP_BA0, and WP_BA60-S, respectively. The observed maximum decrement of

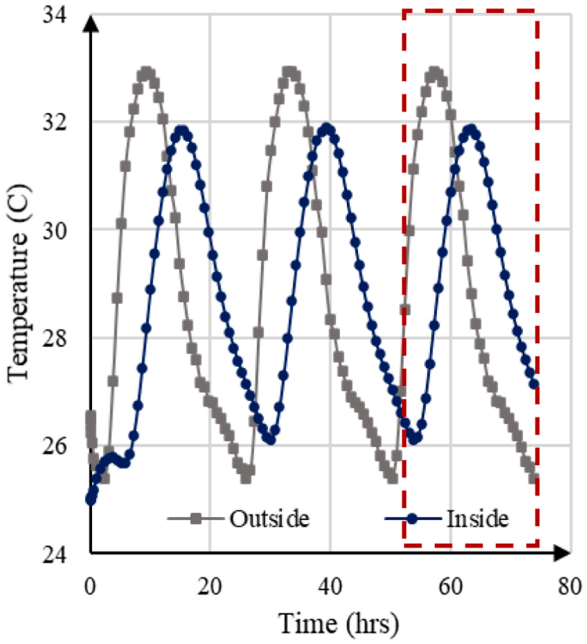

Fig. 13. Temperature variation in the outside surface and inside surface (WP_BA0).

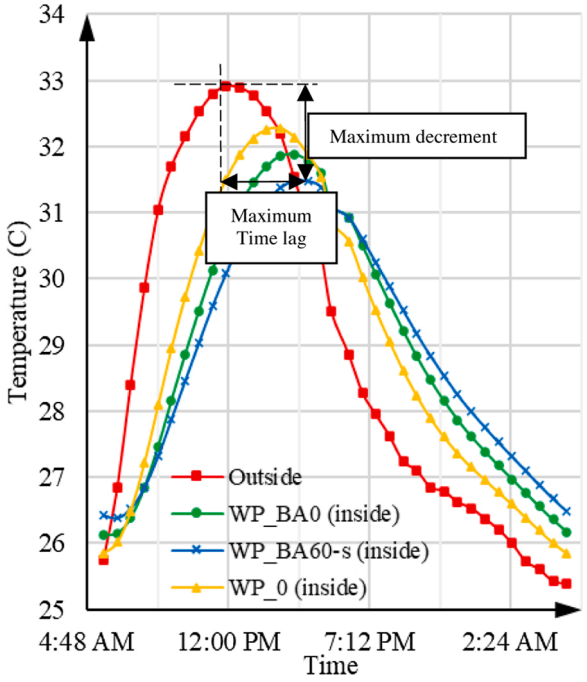

Fig. 14. Temperature variation in the outside surface and inside surface for 24 h period.

temperature for the walls with developed plaster is about 0.5 °C. This is 2% less than the wall plastered with conventional plaster.

7. Parametric study

A parametric study was conducted to predict the effectiveness of newly developed plaster (BA60-S) with changes in thermo sensitive parameters.

7.1. Effect of thickness of the plaster

The selection of the optimum thickness of a thermal insulation layer is a critical parameter which needs to be studied for an economical construction project [35]. A range of thicknesses from 10 mm to 50 mm was considered in this study and the internal temperature variation in WP_BA60-S was observed (Fig. 15). The computed decrement factors and time lags for different thicknesses are plotted in Fig. 16 respect to the plaster thicknesses.

It can be noted that the decrement factor reduces with increasing thickness. The effect of thickness reverses in the change of time lag. The decrement factor varied in the range from 0.79 to 0.51 for the thickness range of 10 mm–50 mm. The noted percentage reduction of internal temperature with respect to the WP_0 was 7%, 13 %, 17 %, 21 %, 25 %, 28 %, 31 %, 36 %, and 40 % for plaster thickness 10 mm, 15 mm, 20 mm, 25 mm, 30 mm, 35 mm, 40 mm, 45 mm, and 50 mm, respectively. Similarly, the noted time lag increments respect to WP_0 was 20 %, 32 %, 47 %, 55 %, 63 %, 75 %, 82 %, 87 %, and 90 % for the walls with 10 mm, 15 mm, 20 mm, 25 mm, 30 mm, 35 mm, 40 mm, 45 mm, and 50 mm, respectively. This shows that the effect of plaster thickness on time lag reduces with increasing thickness. From the results obtained, it was revealed that the walls with higher plaster thickness provide a better thermal comfort within the buildings and the effect of thickness reduces beyond a maximum thickness.

7.2. Effect of environmental temperature

The climatic conditions of the environment also influence the effectiveness of insulation materials. The climatic data among the different regions of the world were collected to understand the heat transfer behavior and assess the feasibility of extending these results for the applications in various part of the world. The environmental temperature of various cold and hot countries on a randomly selected day in July 2020 [36] are listed in Table 9. The heat transfer model developed to predict the behavior in this study was further analyzed for the environmental temperature fluctuations given in Table 9. The methodology stated in Section 7.3 (Fig. 13) was followed in this analysis as well. The average outdoor temperatures and predicted indoor temperatures in both countries are illustrated in Fig. 17.

The computed decrement factors for warm countries and cold countries with the developed plaster are 0.638 and 0.639, respectively which indicates that the developed insulation plaster would be equally utilized in all regions of the world. The noted time lags using the innovate plaster in warm and cold countries were also nearly equal which are 3 h 25 min and 3 h and 20 min, respectively. Based on the obtained decrement factors, it can be proven that the thermal comfort can be enhanced by 12.7 % and 12.4 % in warm and cold countries, respectively.

8. Energy saving

The heat flux through the composite walls were obtained for cold countries and hot countries. Fig. 18 presents the heat flux oscillation throughout a day for a unit wall panel with different plasters in cold and hot countries. The plots show the reduced heat flux in the walls with the developed wall plaster in both climatic conditions. Moreover, the computed annual heat energy consumptions for different climatic conditions are illustrated in Fig. 19. The results indicate that by using the developed plaster in this study, the annual heat loss can be reduced by 16.5 %, and 16.2 % in hot countries and cold countries, respectively. This shows the equal effectiveness of this developed plaster in different climatic conditions. Further, the predicted heat loss reductions can be implied to the annual energy saving of the buildings.

While an average house hold in hot countries use air conditioning to cool down the temperature to 21 °C – 25 °C, a house in a cold country would use heater to raise the temperature to the same level. Thereby, the model was further analyzed during cooling and heating the indoor environment at hot and cold countries, respectively. The corresponding heat fluxes while the indoor environment

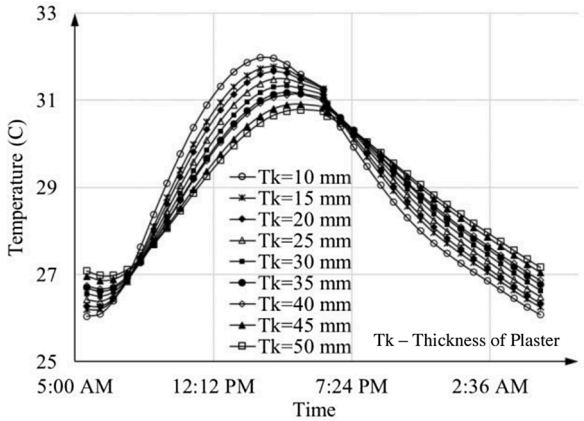

Fig. 15. Effect of plaster thickness on thermal performance of developed composite wall.

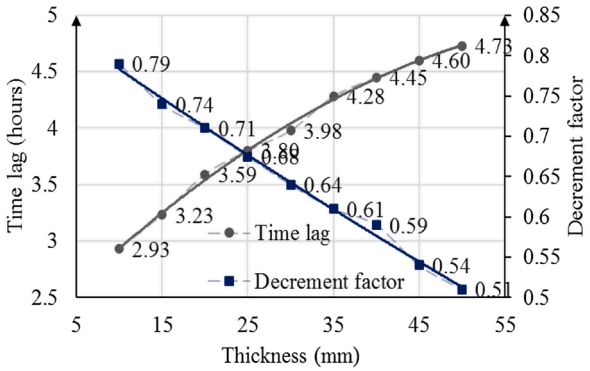

Fig. 16. Effect of plaster thickness on decrement factor and time lag.

Table 9
Climatic data in hot & cold countries.

Time	Hot countries					Cold countries		
	Colombo - Sri Lanka	Paya Lebr-Singapore	New Delhi -India	Tokyo - Japan	New York - USA	London - UK	Minsk - Russia	Zurich - Switzerland
6:00	26.67	26.67	26.67	24.44	23.89	14.44	14.44	13.33
10.00	27.22	28.50	32.00	30.00	27.22	17.78	19.44	18.89
12:00	29.44	31.00	33.00	31.67	30.00	17.78	22.22	21.11
14:00	30.00	30.56	33.50	33.33	31.11	18.89	22.78	22.78
18:00	29.44	30.00	31.00	30.00	30.56	19.44	22.22	21.67
0:00	27.22	28.00	28.00	27.22	26.67	17.22	14.44	17.22

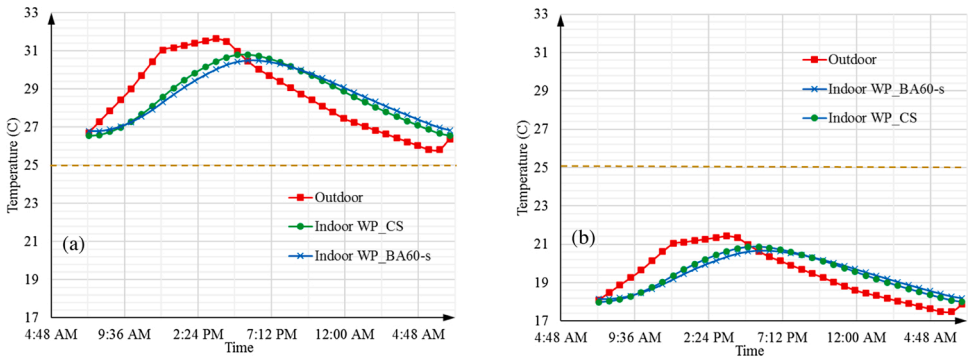

Fig. 17. Effect of innovative plaster (a) In warm countries (b) In cold countries.

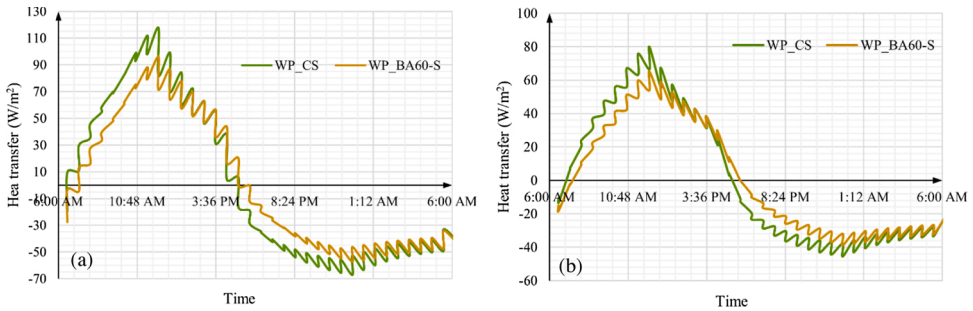

Fig. 18. Predicted heat flux (a) in hot countries (b) in cold countries.

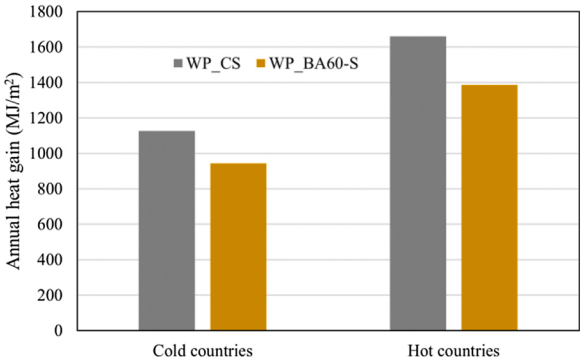

Fig. 19. Annual heat energy consumption.

was kept at 25 °C throughout a day were obtained for both types countries and presented in Fig. 20. The obtained heat fluxes were used to compute the total heat energy in both climatic conditions. Fig. 21 presents the annual heat energy consumptions at both conditions; (a) cooling the indoor environment in hot countries and (b) heating the indoor environment in cold countries. The results show that the annual heat loss can be reduced by 13.3 % and 13.2 % during cooling and heating, respectively. This indicates the ability of developed plaster to minimize either heating or cooling energy requirement in building.

9. Conclusions

This paper presents the development of a cementitious composite plaster by partial replacement of sand by BA. Following conclusions were made:

- The optimum thermo-mechanical performances can be achieved by replacing 60 % wt. of fine aggregates with BA. This helps to minimize the negative effects of the sand mining process for the construction industry, while minimizing the environmental hazard resulting from waste disposal process of BA.
- In the plaster production process using oven dried BA, the water/cement ratio should be maintained less than 1.2 with or without superplasticizer. Otherwise, it adversely affects the compressive strength of plaster.
- The thermal conductivity and compressive strength of developed composite plaster indicated a negatively decreasing trend with increased weight percentage of the BA.
- The optimum thermal performance can be achieved with the plaster containing cement: sand: BA in 1:1.2:1.8 proportion by weight, with the water: cement ratio of 1.2 and 10 mL/Kg of cement superplasticizer (BA60-S).
- The set composite plaster indicated good adherence properties with masonry walls, and no degradation was noted for the outdoor exposure of 2 years to the tropical environment.
- The numerical model developed to predict the heat transfer behavior through the composite wall is in good agreement with theoretical predictions and also with the previous literature.
- A significant effect on decrement factors and time lag was noticed for different wall configurations. The reduction in the decrement factor of the wall panel with conventional plaster was 9%, while it was 20 % in the wall panel with the BA-cement (WP_BA60-S) plaster. And the increment in the time lag of the conventional wall panel was 28 %, while 54 % was noted in the innovative wall panel (WP_BA60-S).
- From the parametric analysis, it was noted that a decrement factor increases from 7% to 70 % and a time lag reduction of 28%–133% can be achieved by providing an appropriate plaster with good thermal properties.

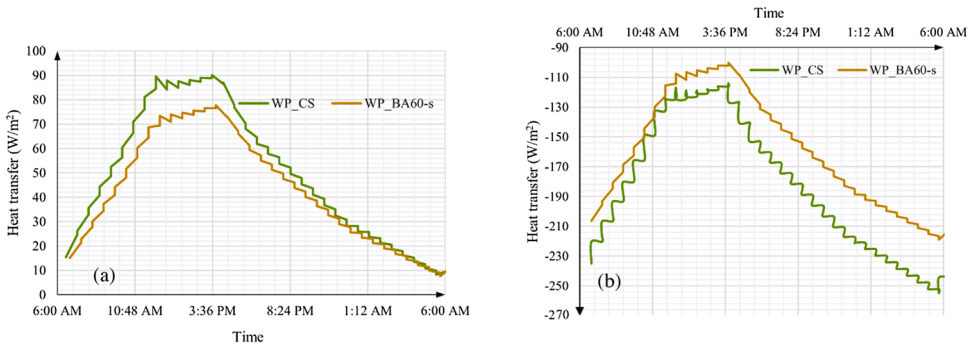

Fig. 20. Predicted heat flux (a) in hot countries during cooling (b) in cold countries during heating.

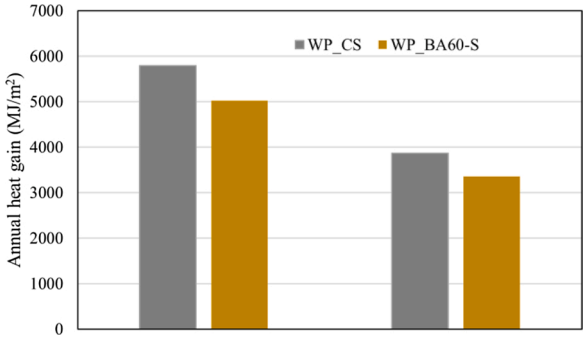

Fig. 21. Annual heat energy consumptions during cooling and heating.

- More than 0.5 °C reduction in internal wall temperature was noted from the walls with developed plaster when compared to conventional cement sand plastered walls. This further indicates the possible reduction of mechanical ventilation or heating in buildings which leads to energy saving with the application of newly developed BA based plaster.
- This study also shows that by using the BA-cement plaster developed in this study, the annual heat losses can be reduced from 16 % to 17 % in any climatic condition either hot or cold. And an average of 13 % energy saving can be expected during cooling and heating using the developed plaster than the conventional plaster.

Data availability

The raw/processed data required to reproduce these findings cannot be shared at this time as the data also forms part of an ongoing study.

CRediT authorship contribution statement

K.A.D.Y.T. Kahandawa Arachchi: Testing, Analysis, Development and preparation of paper. **A. Selvaratnam**: Numerical Modelling, Data interpretation and preparation of paper. **J.C.P.H. Gamage**: Research Supervision, Guidance, Planning and Monitoring. **G.I.P. De Silva**: Research Supervision, Guidance, Planning.

Declaration of Competing Interest

The authors report no declarations of interest.

Acknowledgments

The authors would like to express their sincere gratitude to all the technical staff in Building materials Laboratory and Structural testing laboratory, University of Moratuwa. The financial support provided by National Research Council (Grant no. PPP 18-01) is greatly appreciated.

References

[1] M. Shekarchian, M. Moghavvemi, B. Rismanchi, T.M.I. Mahlia, T. Olofsson, The cost benefit analysis and potential emission reduction evaluation of applying wall insulation for buildings in Malaysia, Renew. Sustain. Energy Rev. 16 (2012) 4708–4718, https://doi.org/10.1016/j.rser.2012.04.045.
[2] S. Evans, R. Pearce, Mapped: The World's Coal Power Plants, 2020. https://www.carbonbrief.org/mapped-worlds-coal-power-plants.
[3] A.K. Mandal, O.P. Sinha, Review on Current Research Status on Bottom Ash: An Indian Prospective, J. Inst. Eng. Ser. A 95 (2014) 277–297, https://doi.org/10.1007/s40030-014-0100-0.
[4] K. Sideris, H. Justnes, T.S. M.Sui, Fly ash. Prop. Fresh Hardened Concr. Contain. Suppl. Cem. Mater., Springer, Cham, 2018, https://doi.org/10.1007/978-3-319-70606-1_2.
[5] M.L. Berndt, Properties of sustainable concrete containing fly ash, slag and recycled concrete aggregate, Constr. Build. Mater. 23 (2009) 2606–2613, https://doi.org/10.1016/j.conbuildmat.2009.02.011.
[6] S.U. Hendawitharana, S.M.A. Nanayakkara, Use of bottom ash from coal fired thermal power plants in production of cellular lightweight concrete, MERCon 2018 - 4th Int. Multidiscip. Moratuwa Eng. Res. Conf. (2018) 209–214, https://doi.org/10.1109/MERCon.2018.8421957.
[7] A.K. Mandal, O.P. Sinha, Production of thermal insulation blocks from bottom ash of fluidized bed combustion system, Waste Manag. Res. 35 (2017) 810–819, https://doi.org/10.1177/0734242X17707575.
[8] P. Aggarwal, Y. Aggarwal, S.M. Gupta, Effect of bottom ash as replacement of fine aggregates in concrete, Asian J. Civ. Eng. (BUILDING HOUSING) 8 (2007) 49–62.
[9] W. Wongkeo, P. Thongsanitgarn, K. Pimraksa, A. Chaipanich, Compressive strength, flexural strength and thermal conductivity of autoclaved concrete block made using bottom ash as cement replacement materials, Mater. Des. 35 (2012) 434–439, https://doi.org/10.1016/j.matdes.2011.08.046.
[10] J.C.P.H. Gamage, R. Al-Mahaidi, M.B. Wong, Effect of insulation on the bond behaviour of CFRP-Plated concrete elements, Proceeding Int. Sysposium Bond Behav. FRP Struct. (BBFS 2005) (2005) 119–123.
[11] P. Torkittikul, T. Nochaiya, W. Wongkeo, A. Chaipanich, Utilization of coal bottom ash to improve thermal insulation of construction material, J. Mater. Cycles Waste Manag. 19 (2017) 305–317, https://doi.org/10.1007/s10163-015-0419-2.

[12] M. Mohit, Y. Sharifi, Thermal and microstructure properties of cement mortar containing ceramic waste powder as alternative cementitious materials, Constr. Build. Mater. 223 (2019) 643–656, https://doi.org/10.1016/j.conbuildmat.2019.07.029.
[13] B. Abu-Jdayil, A.H. Mourad, W. Hittini, M. Hassan, S. Hameedi, Traditional, state-of-the-art and renewable thermal building insulation materials: an overview, Constr. Build. Mater. 214 (2019) 709–735, https://doi.org/10.1016/j.conbuildmat.2019.04.102.
[14] K. Selvaranjan, S. Navaratnam, J.C.P.H. Gamage, J. Thamboo, R. Siddique, Thermal and environmental impact analysis of rice husk ash-based mortar as insulating wall plaster, Constr. Build. Mater. 283 (2021), https://doi.org/10.1016/j.conbuildmat.2021.122744.
[15] K. Selvaranjan, J.C.P.H. Gamage, G.I.P. De Silva, S. Navaratnam, Development of sustainable mortar using waste rice husk ash from rice mill plant: physical and thermal properties, J. Build. Eng. (2021) 102614, https://doi.org/10.1016/j.jobe.2021.102614.
[16] P.L.N. Fernando, M.T.R. Jayasinghe, C. Jayasinghe, Structural feasibility of Expanded Polystyrene (EPS) based lightweight concrete sandwich wall panels, Constr. Build. Mater. 139 (2017) 45–51, https://doi.org/10.1016/j.conbuildmat.2017.02.027.
[17] N.H. Ramli Sulong, S.A.S. Mustapa, M.K. Abdul Rashid, Application of expanded polystyrene (EPS) in buildings and constructions: a review, J. Appl. Polym. Sci. 136 (2019) 1–11, https://doi.org/10.1002/app.47529.
[18] M. Farouk, A.M. Soltan, S. Schlüter, E. Hamzawy, A. Farrag, A. El-Kammar, A. Yahia, H. Pollmann, Optimization of microstructure of basalt-based fibers intended for improved thermal and acoustic insulations, J. Build. Eng. (2020) 101904, https://doi.org/10.1016/j.jobe.2020.101904.
[19] J.L. Niu, L.Z. Zhang, H.G. Zuo, Energy savings potential of chilled-ceiling combined with desiccant cooling in hot and humid climates, Energy Build. 34 (2002) 487–495, https://doi.org/10.1016/S0378-7788(01)00132-3.
[20] N.I.R. Ramzi Hannan, S. Shahidan, N. Ali, M.Z. Maarof, A comprehensive review on the properties of coal bottom ash in concrete as sound absorption material, MATEC Web Conf. 103 (2017) 01005, https://doi.org/10.1051/matecconf/201710301005.
[21] M. Cheriaf, J. Cavalcante Rocha, J. Pera, Pozzolanic properties of pulverized coal combustion bottom ash, Cem. Concr. Res. 29 (1999) 1387–1391, https://doi.org/10.1016/j.conbuildmat.2014.06.034.
[22] F. Batool, M.M. Rafi, V. Bindiganavile, Microstructure and thermal conductivity of cement-based foam: a review, J. Build. Eng. 20 (2018) 696–704, https://doi.org/10.1016/j.jobe.2018.09.008.
[23] A.G. Mal'Chik, S.V. Litovkin, P.V. Rodionov, Investigations of physicochemical properties of bottom-ash materials for use them as secondary raw materials, IOP Conf. Ser. Mater. Sci. Eng. 91 (2015), https://doi.org/10.1088/1757-899X/91/1/012081.
[24] A. Ghosh, A. Ghosh, S. Neogi, Reuse of fly ash and bottom ash in mortars with improved thermal conductivity performance for buildings, Heliyon 4 (2018) e00934, https://doi.org/10.1016/j.heliyon.2018.e00934.
[25] G. Vasudevan, Performance on coal bottom ash in hot mix asphalt, Int. J. Res. Eng. Technol. 02 (2015) 24–33, https://doi.org/10.15623/ijret.2013.0208004.
[26] M. Mcquarrle, Thermal conductivity: VII, Analysis of variation of conductivity with termperature for Al2O3, BeO, and MgO, J. Am. Ceram. Soc. 37 (1954).
[27] ASTM International, ASTM C150 / C150M-19a, Standard Specification for Portland Cement, West Conshohocken, 2019. www.astm.org.
[28] ASTM International, ASTM D7340-07, Standard Practice for Thermal Conductivity of Leather, West Conshohocken, PA, 2018. www.astm.org.
[29] ASTM International, ASTM C109 / C109M-20a, Standard Test Method for Compressive Strength of Hydraulic Cement Mortars, West Conshohocken, PA, 2020. www.astm.org.
[30] ASTM International, ASTM C 270-07, Standard Specification for Mortar for Unit Masonry, 2007, https://doi.org/10.1520/C0270-10.
[31] ASTM C 1437-07, Standard test method for flow of hydraulic cement mortar, ASTM Int. (2009) 6–7.
[32] ABAQUS Analysis User's Guide, 2013 https://doi.org/130.149.89.49:2080/v6.13/.
[33] M. Ozel, C. Ozel, Effects of wall orientation and thermal insulation on time lag and decrement factor, 9th Int. Conf. Heat Transf. Fluid Mech. Thermodyn. (2012) 680–684.
[34] S. Shaik, K.K. Gorantla, A.B.T.P. Setty, Investigation of building walls exposed to periodic heat transfer conditions for green and energy efficient building construction, Procedia Technol. 23 (2016) 496–503, https://doi.org/10.1016/j.protcy.2016.03.055.
[35] A. Selvaratnam, K.A.D.Y.T. Kahandawa Arachchi, J.C.P.H. Gamage, V. Attanayake, Investigation on an effective bond arrangement of insulated CFRP-strengthened flexural members for improved thermo-mechanical performance, Case Stud. Constr. Mater. 14 (2021) e00544, https://doi.org/10.1016/j.cscm.2021.e00544.
[36] Weather Today, (n.d.). https://www.timeanddate.com/weather. (Accessed 30 August 2020).
[37] M. Ozel, K. Pihtili, Optimum location and distribution of insulation layers on building walls with various orientations, Build. Environ. 42 (2007) 3051–3059, https://doi.org/10.1016/j.buildenv.2006.07.025.